

Fractal Geometry in Electromagnetics Applications

- from Antenna to Metamaterials

Wojciech J. Krzysztofik

Abstract – The effectiveness of antenna and other EM devices geometry in terms of lowering or establishing a specific resonant frequency for different structures of fractal geometry is considered. We provide a comprehensive overview of recent developments in the rapidly growing field of modern communication, especially mobile systems. This research revealed unexpected results, which provided additional insight into unique fractal structures. Results of MoM & FDTD - simulation methods of the circuit- and field antenna and metamaterials parameters in comparison with measurements are presented and discussed.

Keywords – Fractal geometry, Multiband antenna, Small printed antenna, Metamaterials, Modern communications.

I. INTRODUCTION

Antenna design is a mature field of research; it is therefore rare that a new approach arises in view of the traditional methods for use into a modern communication systems. In the past, antennas had simple form based on Euclidean geometry. Recent efforts by several researchers around the world to combine fractal geometry with electromagnetic theory have led to a plethora of new and innovative antenna designs. Fractal antennas do not follow the Euclidean geometry design. Their complex structure is built up through replication of a base shape. It has been an intriguing question among electromagnetic community as to what property of fractals, if any, is really useful, especially when it comes to designing fractal shaped antenna elements.

Fractals are abstract objects that cannot be physically implemented. Nevertheless, some related geometries can be used to approach an ideal fractal that are useful in constructing antennas. Usually, these geometries are called pre-fractals or truncated fractals. In other cases, other geometries such as multi-triangular or multilevel configurations can be used to build antennas that might approach fractal shapes and extract some of the advantages that can theoretically be obtained from the mathematical abstractions. In general, the term fractal antenna technology is used to describe those antenna engineering techniques that are based on such mathematical concepts that enable one to obtain a new generation of antennas with some features that were often thought impossible in the mid-1980s.

After all the work carried out thus far, one can summarize the benefits of fractal technology in the following way:

1. Self-similarity is useful in designing multi-frequency antennas, as, for instance, in the examples based on the Sierpinski gasket, and has been applied in designing of multi-band arrays.
2. Fractal dimension is useful to design electrically small antennas, such as the Hilbert, Minkowski and Koch monopoles or loops, and microstrip patch antennas.
3. Mass fractals and boundary fractals are useful in obtaining high-directivity elements, under-sampled arrays, and low-sidelobes arrays.
4. Recently, the space-filling Hilbert (Peano) fractal curves were used to realize the high-impedance ground planes EBG, so called metamaterials, of the high-performance, low-profile, conformal and flush-mounted antennas with improved radiation characteristics for various communications and radar applications.

In many EM devices, the self-similarity and plane-filling nature of fractal geometries are often qualitatively linked to its frequency characteristics, i.e. multi-frequency operation, or small size in low frequency bands.

II. BRIEF BACKGROUND ON FRACTAL GEOMETRY

A. Fractals in Nature

The original inspiration for the development of fractal geometry came largely from an in-depth study of the patterns of nature.

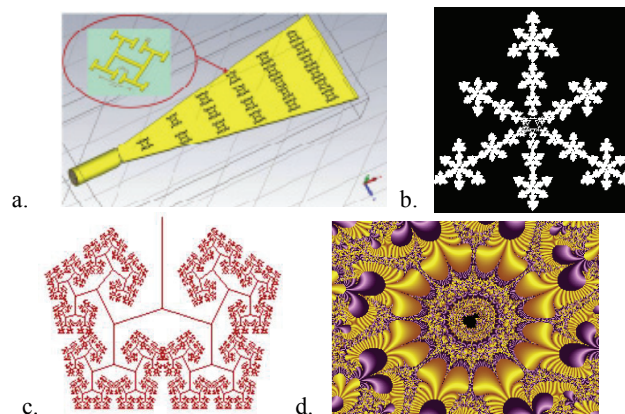


Fig. 1. Fractal objects in nature and technique: fractal cells printed as metamaterial on the septum of GTEM chamber (a), crystal, snowflake (b), the human lungs (c), fractal art (d)

Wojciech J. Krzysztofik is with the Faculty of Electronic Engineering, Wrocław University of Technology, Wybrzeże Wyspiańskiego 27, 50-334 Wrocław, Poland, E-mail: wojciech.krzysztofik@pwr.wroc.pl

and much more (Fig. 1). For millions of years of the evolution, nature has been optimizing the architecture of biological structures to effectively distribute and use energy, and basically a fractal form can be found in every critical structure.

Mandelbrot realized [13] that it is very often impossible to describe nature using only Euclidean geometry that is in terms of straight lines, circles, cubes, and such like. He proposed that fractals and fractal geometry could be used to describe real objects, such as trees, lightning, river meanders and coastlines, to name but a few. Fractal dimension can be non-integers, therefore intuitively, we can represent it as a measure of how much space the fractal occupies. Fractals may be found in nature or generated using a mathematical recipe. The word *fractal* was coined by Benoit Mandelbrot, sometimes referred to as the father of fractal geometry, who said “I coined *fractal* from the Latin adjective *fractus*. The corresponding Latin verb *frangere* means "to break" to create irregular fragments. It is therefore sensible - and how appropriate for our need! - that, in addition to "fragmented" (as in *fraction* or *refraction*), *fractus* should also mean "irregular", both meanings being preserved in fragment” [13]. Moreover he asked: “Why geometry is often described as ‘cold’ or ‘dry’? One reason lies in its inability to describe the shape of a cloud, a mountain, a coastline, or a tree. Clouds are not spheres, mountains are not cones, coastlines are not circles, and bark is not smooth, nor does lightning travel in a straight line.”

To date, there exists no watertight definition of a fractal object. Mandelbrot offered the following definition: “A fractal is by definition a set for which the Hausdorff dimension strictly exceeds the topological dimension”, which he later retracted and replaced with: “A fractal is a shape made of parts similar to the whole in some way”.

So, possibly the simplest way to define a *fractal* is as an object which appears self-similar under varying degrees of magnification, and in effect, possessing symmetry across scale, with each small part of the object replicating the structure of the whole. Some examples of self-similarity are shown in Fig. 2. The rectangular outlining indicates a few of the self-similarities of the object.

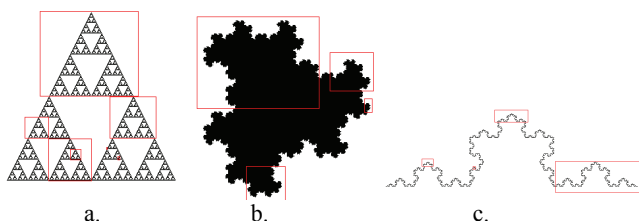


Fig. 2. The self-similar components of different fractals: Sierpinski gasket (a), dragon (b), Koch curve (c)

This is perhaps the loosest of definitions, however, it captures the essential, defining characteristic, that of self-similarity.

But here are five properties which most fractals:

- have detail on arbitrarily small scales,
- are usually defined by simple recursive processes,
- are too irregular to be described in traditional geometric language,
- have some sort of self-similarity

- have fractal dimension.

B. Why Fractal-Shape Antennas ?

Antennas are essentially narrowband devices. Their behaviour is highly dependent on the antenna size to the operating wavelength ratio. This means that for a fixed antenna size, the main antenna parameters (gain, input impedance, pattern shape, secondary lobe level, and distribution) will suffer strong variations when changing the operating frequency. The frequency dependence also implies that an antenna has to keep a minimum size relative to wavelength to operate efficiently. That is, given a particular frequency, the antenna cannot be made arbitrarily small: it usually has to keep a minimum size, typically on the order of a quarter wavelength. These well-known results have been constraining for decades the antenna performance in telecommunication systems, and they have been the object of an intensive research with some successful results. However, the size to wavelength dependence is still a problem in many systems where former antenna designs are not particularly suitable. In that sense, the fractal design of antennas and arrays can help in dealing with the problem by contributing with a huge, rich variety of geometrical shapes with some astonishing properties.

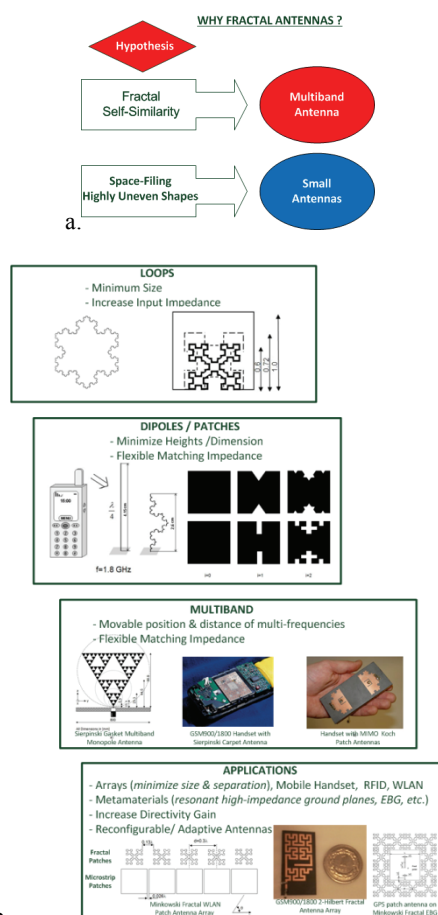


Fig. 3. Why fractal antennas (a), and the various fractal geometry they fall into few main categories: loops, dipoles, multiband fractal patches, antenna arrays, metamaterials (b)

The reason *why* the fractal design of antennas and metamaterials appear as an attractive way to make it is few-fold (Fig. 3). First because one should expect a self-similar antenna (which contains many copies of itself at several scales) to operate in a similar way at several wavelengths. That is, the antenna should keep similar radiation parameters through several bands. Second, because the space-filling properties of some fractal shapes (the fractal dimension) might allow fractally shaped small devices to better take advantage of the small surrounding space.

The fractal design of antennas and arrays results from the blend of two apparently disjoint disciplines, namely electromagnetic theory and geometry. From the early spiral and log-periodic antennas developed in the early sixties by Carrel Mayes et al, and from the works of Benoit Mandelbrot on fractal geometry, the fractal antennas appears as natural way to explore for multi-frequency operation and for an antenna size reduction.

C. How Fractals can be used as Antennas and why Fractals are Space-filling Geometries

While Euclidean geometries are limited to points, lines, sheets, and volumes, fractals include the geometries that fall between these distinctions. Therefore, a fractal can be a line that approaches a sheet. The line can meander in such a way as to effectively almost fill the entire sheet. These space-filling properties lead to curves that are electrically very long, but fit into a compact physical space. This property can lead to the miniaturization of antenna elements.

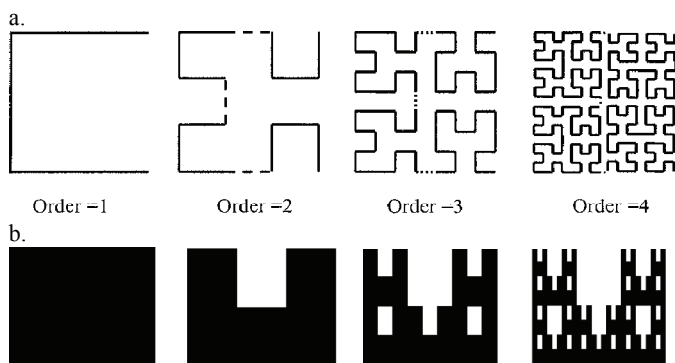


Fig. 4. Generation the four iterations of Hilbert fractal, the space-filling curve (a), and the self-affine fractal multiband antenna (b)

In the previous section, it was mentioned that pre-fractals drop the complexity in the geometry of a fractal that is not distinguishable for a particular application. For antennas, this can mean that the intricacies that are much, much smaller than a wavelength in the band of useable frequencies can be dropped out [8]. This now makes infinitely complex structure, which could only be analysed mathematically, but may not be possible to be manufactured. It will be shown that the band of generating iterations required to reap the benefits of miniaturization is only a few before the additional complexities become indistinguishable. There have been many interesting works that have looked at this emerging field of fractal electrodynamics. Much of the pioneering work in this area has been documented in [9] and [10]. These works

includes fundamentals about the mathematics, as well as studies in fractal antennas and reflections from fractal surfaces.

The space-filling properties of the Hilbert curve and related curves (e.g. Peano fractal) make them attractive candidates for use in the design of fractal antennas. The space-filling properties of the Hilbert curve were investigated in [8] as an effective method for designing compact resonant antennas. The first four steps in the construction of the Hilbert curve are shown in Fig. 4.

The self-affine fractal geometry [11] presented in Fig 4b is constructed by scaling a square by a factor of 3 in the horizontal direction and by a factor of 2 in the vertical direction, giving six rectangles, out of which the central rectangle on the upper side is removed. This is the first iteration. The process is now repeated on the remaining rectangles in the second iteration and can be continued *ad infinitum*. This procedure is known as the iterated function system (IFS).

D. Iterated Function Systems, IFS: The Language of Fractals

Iterated function systems (IFS) represent an extremely versatile method for conveniently generating a wide variety of useful fractal structures [1-7], [12-13]. These iterated function systems are based on the application of a series of affine transformations, w , defined by

$$w \begin{pmatrix} x \\ y \end{pmatrix} = \begin{pmatrix} a & b \\ c & d \end{pmatrix} \begin{pmatrix} x \\ y \end{pmatrix} + \begin{pmatrix} e \\ f \end{pmatrix} \tag{1}$$

or, equivalently, by

$$w(x, y) = (ax + by + e, cx + dy + f), \tag{2}$$

where real number coefficients (a, b, c, d, e, f) are responsible for movement of fractal element in space: a, d - scaling, b, c - rotation by ϕ_1, ϕ_2 angles with respect to axis of coordinating system, and e, f - linear translation by the vector (e, f), respectively, (see Figure 5). They are expressed as:

$$a = \delta_1 \cos \phi_1; \quad d = \delta_2 \cos \phi_2; \quad b = \delta_2 \sin \phi_2; \quad c = \delta_1 \sin \phi_1$$

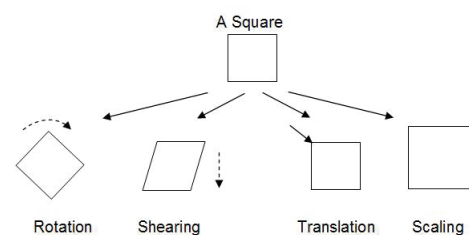


Fig. 5. The affine transforms

Now suppose we consider w_1, w_2, \dots, w_N as a set of affine linear transformations, and let A be the initial geometry. Then a new geometry, produced by applying the set of transformations to the original geometry, A , and collecting the results from $w_1(A), w_2(A), \dots, w_N(A)$, can be represented by

$$W(A) = \bigcup_{n=1}^N w_n(A) \tag{3}$$

where W is known as the Hutchinson operator [1], [12]. A fractal geometry can be obtained by repeatedly applying W to the previous geometry. For example, if the set A_0 represents the initial geometry, then we will have

$$A_1 = W(A_0); \quad A_2 = W(A_1); \quad \dots; \quad A_{k+1} = W(A_k) \tag{4}$$

An iterated function system generates a sequence that converges to a final image, A_∞ , in such a way that

$$W(A_\infty) = A_\infty \tag{5}$$

This image is called the attractor of the iterated function system, and represents a "fixed point" of W .

For the Koch fractal curve (Fig. 2c) the matrix of affine transformation has following form

$$w_q \begin{pmatrix} x \\ y \end{pmatrix} = \begin{pmatrix} \delta_{q1} \cos \theta_{q1} & -\delta_{q2} \sin \theta_{q2} \\ \delta_{q1} \sin \theta_{q1} & \delta_{q2} \cos \theta_{q2} \end{pmatrix} \begin{pmatrix} x \\ y \end{pmatrix} + \begin{pmatrix} t_{q1} \\ t_{q2} \end{pmatrix} \tag{6}$$

and scaling factor is expressed as

$$\delta_q = \frac{1}{2 + 2 \cos \theta_q} \tag{7}$$

where θ_{qi} is the inclination angle of the second subsection with respect to the first, and t_{qi} is an element displacement on the plane. Figure 6 illustrates the iterated function system procedure for generating the well-known Koch fractal curve. In this case, the initial set, A_0 , is the line interval of unit length, i.e., $A_0 = \{x : x \in [0,1]\}$, $\theta_q = 60^\circ$, and $\delta_q = \frac{1}{3}$.

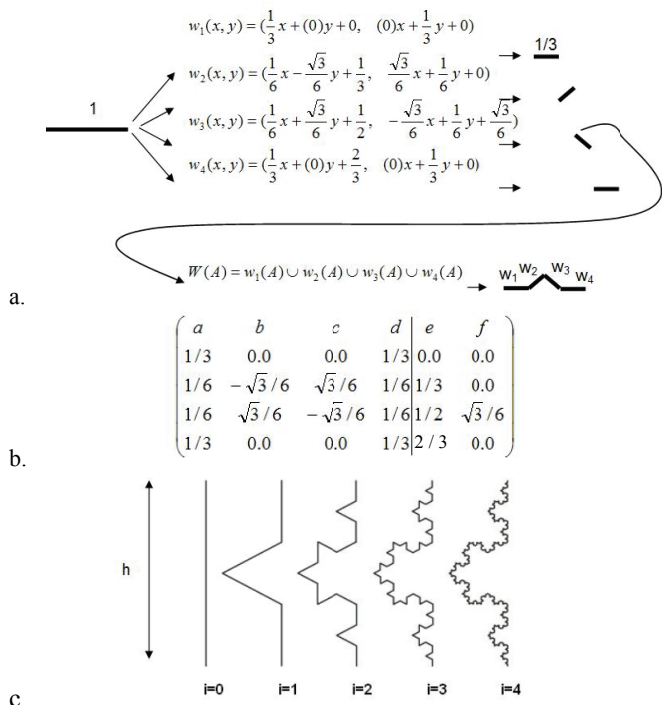


Fig. 6. The fractal Koch curve as an iterated function system (a), the affine transformation matrices (b), and the first 4-stages in the construction of it (c)

TABLE 1
COLLECTION OF SOME FRACTAL STRUCTURES USEFUL FOR ANTENNA AND METAMATERIALS APPLICATIONS

| Fractal Type | Similarity Dimension | Iterated Function System | Sketch of Iterated Structure |
|---------------------|----------------------|--|------------------------------|
| Koch Curve | 1.2618 | $w_1(x, y) = \left[\frac{1}{3}x; \frac{1}{3}y\right]$ $w_2(x, y) = \left[\frac{1}{6}x - \frac{\sqrt{3}}{6}y + \frac{1}{3}; \frac{\sqrt{3}}{6}x + \frac{1}{6}y\right]$ $w_3(x, y) = \left[\frac{1}{6}x + \frac{\sqrt{3}}{6}y + \frac{1}{2}; -\frac{\sqrt{3}}{6}x + \frac{1}{6}y + \frac{\sqrt{3}}{6}\right]$ $w_4(x, y) = \left[\frac{1}{3}x + \frac{2}{3}; \frac{1}{3}y\right]$ | |
| Koch Snowflake | 2 | $w_1(x, y) = \left[\frac{1}{3}x - \frac{\sqrt{3}}{6}y; \frac{\sqrt{3}}{6}x + \frac{1}{2}y\right]$ $w_2(x, y) = \left[\frac{1}{3}x + \frac{1}{\sqrt{3}}; \frac{1}{3}y + \frac{1}{3}\right]$ $w_3(x, y) = \left[\frac{1}{3}x; \frac{1}{3}y + \frac{2}{3}\right]$ $w_4(x, y) = \left[\frac{1}{3}x - \frac{1}{\sqrt{3}}; \frac{1}{3}y + \frac{1}{3}\right]$ $w_5(x, y) = \left[\frac{1}{3}x + \frac{\sqrt{3}}{3}; \frac{1}{3}y - \frac{1}{3}\right]$ $w_6(x, y) = \left[\frac{1}{3}x; \frac{1}{3}y - \frac{2}{3}\right]$ $w_7(x, y) = \left[\frac{1}{3}x + \frac{1}{\sqrt{3}}; \frac{1}{3}y - \frac{1}{3}\right]$ | |
| Minkowski Curve | 1.5 | $w_1(x, y) = \left[\frac{1}{4}x; \frac{1}{4}y\right]$ $w_2(x, y) = \left[-\frac{1}{4}y + \frac{1}{4}; \frac{1}{4}x\right]$ $w_3(x, y) = \left[\frac{1}{4}x + \frac{1}{4}; \frac{1}{4}y + \frac{1}{4}\right]$ $w_4(x, y) = \left[-\frac{1}{4}y + \frac{1}{4}; \frac{1}{4}x + \frac{1}{4}\right]$ $w_5(x, y) = \left[-\frac{1}{4}y + \frac{1}{4}; \frac{1}{4}x\right]$ $w_6(x, y) = \left[\frac{1}{4}x + \frac{1}{4}; \frac{1}{4}y - \frac{1}{4}\right]$ $w_7(x, y) = \left[-\frac{1}{4}y + \frac{3}{4}; \frac{1}{4}x - \frac{1}{4}\right]$ $w_8(x, y) = \left[\frac{1}{4}x + \frac{3}{4}; \frac{1}{4}y\right]$ | |
| Hilbert Curve | 1.2619 | $w_1(x, y) = \left[\frac{1}{2}y - \frac{1}{2}; -\frac{1}{2}x\right]$ $w_2(x, y) = \left[\frac{1}{2}x - \frac{1}{2}; \frac{1}{2}y + \frac{1}{2}\right]$ $w_3(x, y) = \left[\frac{1}{2}x + \frac{1}{2}; \frac{1}{2}y + \frac{1}{2}\right]$ $w_4(x, y) = \left[-\frac{1}{2}y - \frac{1}{2}; \frac{1}{2}x - \frac{1}{2}\right]$ | |
| Sierpinski Gasket | 1.5849 | $w_1(x, y) = \left[\frac{1}{2}x; \frac{1}{2}y\right]$ $w_2(x, y) = \left[\frac{1}{2}x + \frac{1}{2}; \frac{1}{2}y\right]$ $w_3(x, y) = \left[\frac{1}{2}x + \frac{1}{4}; \frac{1}{2}y + \frac{\sqrt{3}}{4}\right]$ | |
| Sierpinski Carpet | 1.8927 | $w_1(x, y) = \left[\frac{1}{3}x; \frac{1}{3}y\right]$ $w_2(x, y) = \left[\frac{1}{3}x; \frac{1}{3}y + \frac{1}{3}\right]$ $w_3(x, y) = \left[\frac{1}{3}x; \frac{1}{3}y + \frac{2}{3}\right]$ $w_4(x, y) = \left[\frac{1}{3}x + \frac{1}{3}; \frac{1}{3}y\right]$ $w_5(x, y) = \left[\frac{1}{3}x + \frac{2}{3}; \frac{1}{3}y + \frac{1}{3}\right]$ $w_6(x, y) = \left[\frac{1}{3}x + \frac{2}{3}; \frac{1}{3}y + \frac{2}{3}\right]$ $w_7(x, y) = \left[\frac{1}{3}x + \frac{1}{3}; \frac{1}{3}y + \frac{2}{3}\right]$ $w_8(x, y) = \left[\frac{1}{3}x + \frac{1}{3}; \frac{1}{3}y\right]$ | |
| Sierpinski Pentagon | 1.6722 | $w_1(x, y) = [0.382x; 0.382y]$ $w_2(x, y) = [0.382x + 0.618; 0.382y]$ $w_3(x, y) = [0.382x + 0.809; 0.382y + 0.588]$ $w_4(x, y) = [0.382x + 0.309; 0.382y + 0.951]$ $w_5(x, y) = [0.382y - 0.191; 0.382y + 0.588]$ | |
| Fractal Tree | 1.5849 | $w_1(x, y) = \left[\frac{1}{3}x; \frac{1}{3}y + 2\right]$ $w_2(x, y) = \left[\frac{1}{3}x - \frac{4}{3}; \frac{1}{3}y + 2\right]$ $w_3(x, y) = \left[\frac{1}{3}x + \frac{4}{3}; \frac{1}{3}y + 2\right]$ | |
| Cantor Set | 0.6309 | $w_1(x, y) = \left[\frac{1}{3}x; \frac{1}{3}y - W\right]$ $w_2(x, y) = \left[\frac{1}{3}x + \frac{2}{3}; \frac{1}{3}y - W\right]$ | |

Next, the results of these four linear transformations are combined together to form the first iteration of the Koch curve, denoted by A_1 . The second iteration of the Koch curve, A_2 , may then be obtained by applying the same four affine transformations to A_1 . Higher-order version of the Koch curve is generated by simply repeating the iterative process until the desired resolution is achieved. The first four iterations of the Koch curve, are shown in Fig. 6c.

In Table 1 the collection of basic fractal structures, especially suited for small low frequency or multi-frequency operated antennas and metamaterials are presented.

E. Self-Affine Sets

Self-affine sets form an important class of sets, which include self-similar sets as a particular case. An affine transformation $S: \mathfrak{R}^n \rightarrow \mathfrak{R}^n$ is a transformation of the form [1]

$$w(x, y) = T(x, y) + t \quad (8)$$

where T is a linear transformation on \mathfrak{R}^n (which may be represented by an $n \times n$ matrix) and t is a vector in \mathfrak{R}^n . Thus an affine transformation w is a combination of a translation, rotation, dilation and, perhaps reflection (e.g. see Figure 4b). In particular, w maps spheres to ellipsoids, squares to parallelograms, etc. Unlike similarities, affine transformations contract with differing ratios in different directions.

If w_1, \dots, w_m are self-affine contractions on \mathfrak{R}^n , the unique compact invariant set F for the w_i is termed a self-affine set. An example is given in Figure 5: w_1, w_2 and w_3 are defined as the transformations that map the line segment onto the three line segments in the obvious way. It is naturally to look for a formula for the dimension of self-affine sets that generalizes formula for self-similar sets. We would hope that the dimension depends on the affine transformations in a reasonably simple way, easily expressible in terms of the matrices, and vectors that represent the affine transformation. Unfortunately, the situation is much more complicated than this. If the affine transformations are varied in a continuous way, the dimension of the self-affine set need not change continuously. With such discontinuous behaviour, which becomes worse for more involved sets of affine transformations, it is likely to be difficult to obtain a general expression for the dimension of self-affine sets.

F. The Fractal Dimensions

Generally, we can conceive of objects that are zero dimensional or 0D (points), 1D (lines), 2D (planes), and 3D (solids). We feel comfortable with zero, one, two and three dimensions. We form a 3D picture of our world by combining the 2D images from each of our eyes. Is it possible to comprehend higher-dimensional objects, i.e. 4D, 5D, 6D and so on? What about non-integer-dimensional objects such as 2.12D, 3.79D or 36.91232 ... D? Methods of classical geometry and calculus are unsuited to studying fractals and we need alternative techniques. There are many definitions of fractal dimension [12] and we shall encounter a number of them as we proceed through the text [1], including: the similarity dimension, DS ; the divider dimension, DD ; the

Hausdorff dimension, DH ; the box counting dimension, DB ; the correlation dimension, DC ; the information dimension, DI ; the point wise dimension DP ; the averaged point wise dimension, DA ; and the Lyapunov dimension DL . The last seven dimensions listed are particularly useful in characterizing the fractal structure of strange attractors associated with chaotic dynamics.

So, the main tool for fractal geometry is the dimension in its many forms. Very roughly, a dimension provides a description of how much space a set fills. It is a measure of the prominence of irregularities of a set when viewed at very small scales. A dimension contains much information about the geometrical properties of a set.

One of the most important in classifying fractals is the Hausdorff dimension [12]. In fact, Mandelbrot suggested that a fractal may be defined as an object which has a Hausdorff dimension which exceeds its topological dimension. A complete mathematical description of the Hausdorff dimension is outside the scope of this text [1]. In addition, the Hausdorff dimension is not particularly useful to the engineer or scientist hoping to quantify a fractal object, the problem being that it is practically impossible to calculate it for real data. We therefore begin this section by concentrating on the closely related box counting dimension DB and its application to determining the fractal dimension of natural fractals.

The Box-Counting or Box Dimension, DB , is one of the most widely used dimension [12]. Its popularity is largely due to its relative ease of mathematical calculation and empirical estimation. The definition goes back at least to the 1930s and it has been variously termed Kolmogorov entropy, entropy dimension, metric dimension, etc. We shall always refer to box or box counting dimension to avoid confusion.

Let F be any non-empty bounded subset of \mathfrak{R}^n (in n -dimensional Euclidian space \mathfrak{R}^n) and let $N_\delta(F)$ be the smallest number of sets of diameter at most δ which can cover F . The box-counting dimension or box dimension of F is defined as

$$DB(F) = \lim_{\delta \rightarrow 0} \frac{\log N_\delta(F)}{-\log \delta} \quad (9)$$

There are several equivalent definitions of box dimension that are sometimes more convenient to use.

To examine a suspected fractal object for its box counting dimension we cover the object with covering elements or 'boxes' of side length δ . The number of boxes, N , required to cover the object is related to δ through its box counting dimension, DB . The method for determining DB is illustrated in the simple example, where a straight line (a one-dimensional object) of unit length is probed by cubes (3D objects) of side length δ . We require N cubes (volume δ^3) to cover the line. Similarly, if we had used squares of side length δ (area δ^2) or line segments (length δ^1), we would again have required N of them to cover the line. Equally, we could also have used 4D, 5D, or 6D elements to cover the line segment and still required just N of them. In fact, to cover the unit line segment, we may use any elements with dimension greater than or equal to the dimension of the line itself, namely one. To simplify matters, the line is specified as exactly one unit in length. The number of cubes, squares or

line segments we require to cover this unit line is then $N\delta = 1$, hence $N = 1/\delta$. Notice that the exponent of δ remains equal to one regardless of the dimension of the probing elements, and is in fact the box counting dimension, DB , of the object under investigation. Notice also that for the unit (straight) line, the Euclidean-, the box-, and the topological-dimension, are equal each other, $DE=DB=DT (= 1)$, hence it is not a fractal by our definition in section II.A, as the fractal dimension, here given by DB , does not exceed the topological dimension, DT . The Box-counting dimension, DB , is widely used as a measure of pictures that are not self-similar (most real-life case). In the remaining parts of this chapter we will concentrate on the similarity dimension, denoted DS , to characterize the construction of regular fractal objects.

The Similarity Dimension, DS , is the key structural parameter describing the self-similar fractals and is defined by partitioning the volume where the fractal lies into boxes of side δ . We hope that over a few decades in δ , the number of boxes that contain at least one of the discharge elements will scale as

$$N(\delta) \sim \delta^{-D}. \quad (10)$$

The concept of dimension is closely associated with that of scaling. Consider the line, surface and solid, divided up respectively by self-similar sub-lengths, sub-areas and sub-volumes of side length δ . For simplicity in the following derivation assume that the length, L , area, A , and volume, V , are all equal to unity. Consider first the line. If the line is divided into N smaller self-similar segments, each δ in length, then δ is in fact the scaling ratio, i.e. $\delta/L = \delta$, since $L = 1$. Thus $L = N\delta = 1$ i.e. the unit line is composed of N self-similar parts scaled by $\delta = 1/N$.

Now consider the unit area. If we divide the area again into N segments each δ^2 in area, then $A = N\delta^2 = 1$ i.e. the unit surface is composed of N self-similar parts scaled by $\delta = 1/N^{1/2}$. Applying similar logic, we obtain for a unit volume $V = n\delta^3 = 1$ i.e. the unit solid is N self-similar parts scaled by $\delta = 1/N^{1/3}$. Examining above expressions we see that the exponent of δ in each case is a measure of the (similarity) dimension of the object, and we have in general

$$N\delta^{-DS} = 1 \quad (11)$$

Using logarithms leads to the expression,

$$DS = \frac{\log(N)}{\log(1/\delta)} \quad (12)$$

Note that here the letter 'S' denotes the similarity dimension.

The above expression has been derived using familiar objects which have the same integer Euclidean, topological and similarity dimensions, i.e. a straight line, planar surface and solid object, where $DE = DS = DT$. However, equation (12) may also be used to produce dimension estimates of fractal objects where DS is non-integer. This can be seen by applying the above definition of the self-similar dimension to the triadic Cantor set [1]. We saw that the left-hand third of the set contains an identical copy of the set. There are two such identical copies of the set contained within the set, thus $N=2$ and $\delta=1/3$. According to equation (12) the similarity dimension is then

$$DS = \frac{\log(2)}{\log(1/(1/3))} = \frac{\log(2)}{\log(3)} = 0.6309\dots$$

Thus, for the Cantor set, DS is less than one and greater than zero: in fact it has a non-integer similarity dimension of 0.6309... due to the fractal structure of the object. We saw in the previous section that the Cantor set has Euclidean dimension of one and a topological dimension of zero, thus $DE > DS > DT$. The DS dimensions of all representative fractals are introduced in Table 1.

III. SOME USEFUL GEOMETRIES FOR FRACTAL ANTENNA ENGINEERING

Having seen the geometric properties of fractal geometry, it is interesting to explain what benefits are derived when such geometry is applied to the antenna field. Fractals are abstract objects that cannot be physically implemented. Nevertheless, some related geometries can be used to approach an ideal fractal that are useful in constructing antennas. Usually, these geometries are called prefractals or truncated fractals. In other cases, other geometries such as multi-triangular or multilevel configurations can be used to build antennas that might approach fractal shapes and extract some of the advantages that can theoretically be obtained from the mathematical abstractions. In general, the term fractal antenna technology is used to describe those antenna engineering techniques that are based on such mathematical concepts that enable one to obtain a new generation of antennas with some features that were often thought impossible in the mid-1980s.

After all the work carried out thus far, one can summarize the benefits of fractal technology in the following way:

1. Self-similarity is useful in designing multi-frequency antennas, as, for instance, in the examples based on the Sierpinski gasket, fractal tree, Cantor set, and has been applied in designing of multi-band antennas and arrays.
2. Fractal self-filing reduces overall dimension is useful to design electrically small antennas, such as the Hilbert, Peano, Minkowski and Koch monopoles or loops, and fractally shaped microstrip patch antennas.
3. Mass fractals and boundary fractals are useful in obtaining high-directivity elements, under-sampled arrays, and low-sidelobes arrays.

Apparently, the earliest published reference to use the terms fractal radiators and fractal antennas to denote fractal-shaped antenna elements appeared in May, 1994 [14].

A. Fractal as Wire Antenna Elements

The application of fractal geometry to the design of wire antenna elements was first reported in a series of articles by Cohen [15]. These articles introduce the notion of fractalizing the geometry of a standard dipole or loop antenna. This was accomplished by systematically bending the wire in a fractal way, so that the overall arc length remains the same, but the size is correspondingly reduced with the addition of each successive iteration. It has been demonstrated that this approach, if implemented properly, can lead to efficient miniaturized antenna designs (e.g. see Fig. 8).

Fractal Loop Antennas

For instance, the radiation characteristics of Minkowski dipoles and loops were investigated in [16].

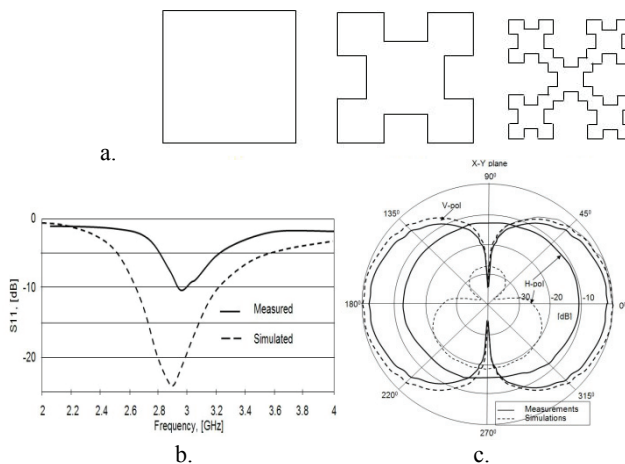


Fig. 7. Minkowski fractal loop antenna (a), the input match (b) and far-field pattern of first-order iteration [6]

The space-filling abilities of fractals fed as loop antennas can exhibit two benefits over Euclidean antennas. The first benefit is that the increased space-filling ability of the fractal loop means that more electrical length can be fitted into a smaller physical area. The increased electrical length leads to a lower resonant frequency, which effectively miniaturizes the antenna. The second benefit is that the increased electrical length can raise the input resistance of a loop antenna when it is used in a frequency range as a small antenna. It can be shown that the resistance increase resulting from the increased wire length for a material with a finite conductivity is insignificant in relationship to the miniaturization of the antenna. The perimeter C length of the fractal is given by the following equation:

$$C_i = \left(1 + \frac{2}{3}w\right)^i \cdot C_{i-1} \quad (13)$$

where i is the number of generating iterations, and w is a indentation width.

Because the term inside the parentheses is greater than one, the perimeter of the fractal grows exponentially with increasing iterations. It can be assumed that as the number of generating iterations is increased, the dimension increases from a one-dimensional line to the dimension calculated of the ideal fractal. Thus, the increase in the iterations increases the fractal dimension, which lowers the resonant frequency. Two iterations of the loop were fabricated [16] to be resonant at the same frequency, and measured. They are fed at the corner via coax through a bazooka balun. The scaling factor of the indentation width is 0.5 for the fabricated geometry. This geometry exhibits a 15% reduction in height from the square loop to the prefractal loop at identical resonances.

Fractal Dipole and Monopole Antennas

An interesting study of the space-filling properties of fractal antennas is to investigate fractal dipole antennas. Three types of Koch fractals were compared as dipoles. They are depicted in Fig. 6c and in Table 1, for the first stages of growth.

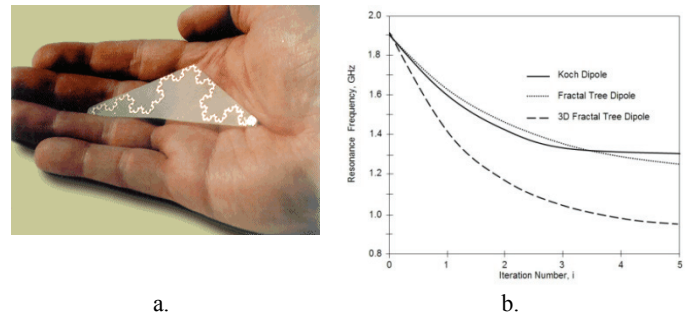


Fig. 8. An example of printed on microwave laminate fractal Koch dipole (a), and the computed [16] resonant frequencies for three types of fractal dipole Koch, 2-D and 3-D trees as a function of number of iterations used in the generating procedure (b)

They included a Koch curve, and a fractal trees. The starting structure for each of the fractals was the same dipole antenna of height h . The Koch dipole has been extensively analyzed in [17]. Also, a version of a tree fractal has been studied in [18]. As mentioned in the previous section, the Koch curve is generated by replacing the middle third of each segment with two sides of an equilateral triangle. The resulting curve is comprised of four segments of equal length. As calculated above, the fractal dimension of the Koch curve is 1.2619. The fractal tree is similar to a real tree, in that the top of every branch splits into more branches. The planar version of the tree has the top third of every branch split into two sections. All the branches split with 60° between them. The length of each path remains the same, in that a path walked from the base of the tree to the tip of a branch would be the same length as the initiator. The dimension DS of fractal tee planar version is equal to 1.395. Lowering the resonant frequency has the same effect as miniaturizing the antenna at a fixed resonant frequency. It can be seen how the planar structures have a similar miniaturization response. Switching to the non-planar three-dimensional version increases this effect. However, it can be seen that the benefits of using fractals to miniaturize are realized within the first several iterations.

Along with looking at the resonant frequency of this antenna, it is also quite interesting to look at the quality factor for these antennas [1], [16]. Computing the quality factor of fractal wire-dipole antennas can show how fractals fill space in a more efficient manner than linear dipoles, and therefore have a lower Q . The Q decreases as the number iterating generations increases for the fractals, as would be expected. Each increasing generating iteration brings the geometry away from the linear, one-dimensional dipole, and closer to the ideal fractal.

B. Fractal Patch Antenna Elements

Fractals can be used to miniaturize patch elements as well as wire elements. The same concept of increasing the electrical length of a radiator can be applied to a patch element [1]-[7], [16]. The patch antenna can be viewed as a microstrip transmission line. Therefore, if the current can be forced to travel along the convoluted path of a fractal instead of a straight Euclidean path, the area required to occupy the

resonant transmission line can be reduced. This technique has been applied to patch antennas in various forms.

One of the fractal structure was discovered in 1916, by a Polish mathematician Waclaw Sierpinski. The Sierpinski sieve of triangles possesses a certain multiband behaviour owing to its self-similar shape, where a monopole antenna based of the Sierpinski gasket has been shown to be an excellent candidate for multiband applications.

A multi-band fractal monopole antenna [19], based on the Sierpinski gasket, was first introduced by Puente et al. [20]. The original Sierpinski monopole antenna is illustrated in Fig. 9.

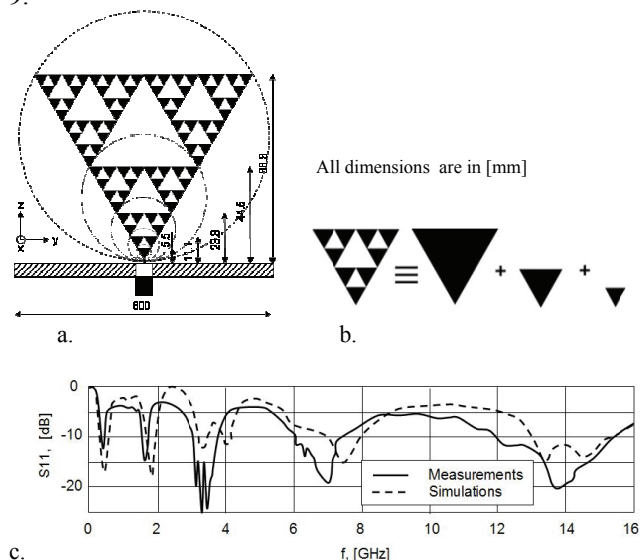


Fig. 9. Five-iteration Sierpinski fractal monopole (a), second iteration Sierpinski gasket as equivalent to an array of tree triangular antennas (b), and the input reflection coefficient, S_{11} relative to 50 ohm (c)

From an antenna engineering point of view, a useful interpretation of Fig. 9a is that the dark triangular areas represent a metallic conductor, whereas the white triangular areas represent regions where metal has been removed. With a few exceptions (especially the log-periodic), we typically use a single antenna (size) for each application (frequency band) as depicted in Figure 9b, so in this case we have the three-in-one compact antenna. Geometry of Sierpinski gasket fractal antenna is fully determined by four parameters, namely, the height h of triangle, the flare angle α , the iteration number i , and the scaling factor δ . As it was described in [20], the Sierpinski monopole presents a log-periodic behaviour [2], [5], [21] (Fig. 9c), with the bands approximately spaced by a factor $\delta = 2$, the antenna keeps a notable degree of similarity through the bands, with a moderate bandwidth (21%). In this case, the antenna geometry is in the form of a classical Sierpinski gasket, with a flare angle of $\alpha = 60^\circ$ and a self-similarity scale factor is determined by ratio of triangle heights of successive iterations, $\delta = h_i / h_{i+1} = 2$. To get a better insight on the log-periodic behaviour of the antenna, the input impedance is also shown in a semi logarithmic scale (Fig. 9c). It can be seen that the antenna is matched approximately at frequencies [1] – [3], [20], [21]:

$$f_{r,i} = 0,3 \cdot \cos\left(\frac{\alpha}{2}\right) \cdot \sqrt{\frac{2,5}{\epsilon_r}} \cdot \frac{c}{h} \delta^i \quad (14)$$

where c is the speed of light in vacuum, h is the height of the largest gasket, δ the log period scaling factor, and i - a natural number of iterations, and ϵ_r is the permittivity of the antenna substrate.

Anyway, such a behaviour is clearly different to that of the bow-tie monopole, which has the first minimum VSWR at $h/\lambda = 0,17$ and the corresponding higher order modes periodically spaced by a frequency gap of $\Delta f = 0,44 c/h$ Hz [21] that is

$$f_r = \frac{2c}{3a\sqrt{\epsilon_r}} \sqrt{m^2 + mn + n^2} \quad (15)$$

where a is the side length of the equally-sided triangle, m, n are numbers of EM-field modes generated in the structure, and c, ϵ_r - as in (14).

The second match of the bow-tie antenna is always better than the any one of higher mode ($S_{11} > 15$ dB as opposed to 8 dB), which might suggest that it can have a more significant effect on the Sierpinski behaviour.

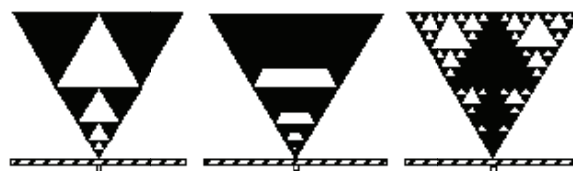


Fig. 10. Modifications of Sierpinski gasket and the related multi-band monopole antennas [22]

To reduce the height of the Sierpinski monopole, a solution is provided to control the spacing between the first two bands. This scheme was subsequently presented in [2], [5], [20]. It was demonstrated that the positions of the different bands can be controlled by proper adjustment of the scale factor δ used to generate the Sierpinski antenna. Further investigations pertaining to improvement of performance of Sierpinski-gasket monopoles through perturbations in their geometry were reported in [1]-[6], [23]. It was found that a variation in the flare angle of the antenna translated into a shift of the operating bands, as well as into a change of the input impedance and radiation patterns. In this approach, the large flare angles and application of affine transformation (Fig. 10) have been used to achieve the desired spacing between the bands, however, at the cost of shallow resonance and decreased bandwidth. Specific applications of these designs to emerging GSM, DECT, WLAN, UMTS, etc. technologies were discussed. The multi-band properties of fractal monopoles based on the generalized family of mod-p Sierpinski gaskets were investigated by Krzysztofik et al. [2], [5]. The advantage of this approach is that it provides a high degree of flexibility in choosing the number of bands and the associated band spacing for a candidate antenna design.

The modified Sierpinski gasket monopole antennas investigated in the paper [2] were designed for dual band WLAN 2.4/5.2 and GSM 900/1800 (see Fig. 11) wireless devices (e.g. computer PCMCIA card, handset board, etc.). The shape of it was introduced for the first time for indoor GSM 900/1800 access point applications in. It has the

dimensions of a computer PCMCIA card whereas the dimensions of the ground plane are 54 by 88.28 mm. The antenna system consists of two metallic layers with the antenna printed on the top side, over the ground plane at the bottom of the PCB. The thickness of each of the copper layers is 35 μ m. The monopole is printed on a double-sided 8-mils thick TACONIC RF-30 substrate, with relative permittivity $\epsilon_r = 3.0$ and loss tangent, $\tan\delta = 0.0018$. The antenna element is printed on a section of dielectric microwave laminate extending beyond the circuitry of the devices. The modified Sierpinski gasket monopole has the ability to handle both the 2.4 and 5.2 GHz ISM bands with a single microstrip feed and without the need for a matching network.

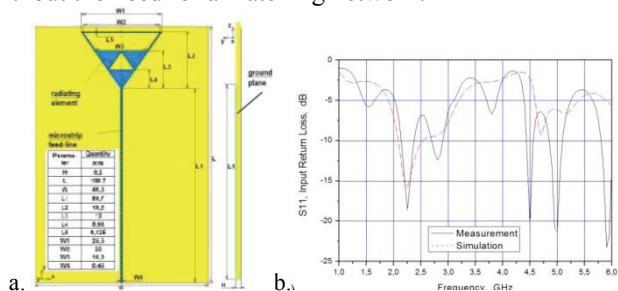


Fig. 11. Modified Sierpinski fractal antennas for GSM 900/1800 (b) applications, and its simulated and measured input reflection coefficient (b) [1], [2]

In order to overcome the problem of miniature microstrip antennas, that is, small bandwidth and radiation efficiency, parasitic techniques have been combined with fractal techniques to obtain miniature and wideband antennas with improved efficiency. A modified Sierpinski-based microstrip antenna consisting of an active patch and a parasitic patch is presented in [23]. Using such a geometry, the resonant frequency of the antenna is 1.26GHz while it is 2GHz for the filled version. By adding the parasitic patch, the bandwidth with respect to the single active element is increased by a factor of 15, resulting in a bandwidth of $BW=2.7\%$ at $SWR=2:1$; the radiation efficiency for this antenna is 84%.

As it was mentioned many times, important characteristic of many fractal geometries is their plane-filling nature. Antenna size is a critical parameter because antenna behaviour depends on antenna dimensions in terms of wavelength (λ). In many applications, space is a constraint factor, therefore an antenna cannot be comparable to the wavelength but smaller (i.e., a small antenna). An antenna is said to be small when its larger dimension is less than twice the radius of the radian sphere; its radius is $\lambda/2\pi$ [1]. Wheeler and Chu were the first who investigated the fundamental limitations of such antennas. The Hilbert and Koch fractal curves have also been useful in designing small microstrip patch antennas. The goal of this section is to present the miniature features of the Hilbert shaped patches and compare it with the Koch shaped patches. Some new advancements are also presented.

Jaroniek [24] have proposed the new PIFA for handset applications, with patch made in the form of Hilbert fractal meander. The antenna geometry conforming to the Hilbert profile effectively increases the length of the current flow path

making it possible to develop a miniature antenna. Since to achieve dual-band performance at least two branches of a radiating element are needed as is shown in Fig. 12.

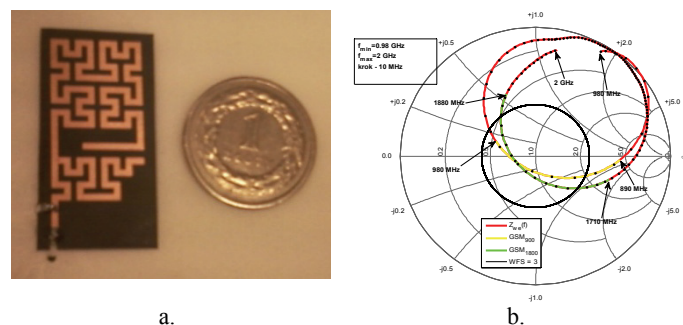


Fig. 12. Dual-band GSM 900/1800 miniaturized Hilbert fractal PIFA photo (a), and impedance plot on Smith chart (b) [24]

An antenna consisting of two Hilbert elements as shown in Fig. 12 was constructed for GSM 900/1800 handset. The smaller element near the feedpoint is responsible for resonance in the high frequency band while the larger element is responsible for the resonance in the low. The models of each element were constructed following a second-order Hilbert curve. Antenna was designed, simulated and manufactured on the one-sided microwave laminate DUROID-5880 ($h_s = 0.125$ mm, $\epsilon_r = 2.2$, $\tan\delta = 0.009$), placed on the ROHACELL 51 IG/A foam ($h_f = 9$ mm, $\epsilon_r = 1.071$, $\tan\delta = 0.0031$). This geometry occupies only about 50% of the volume (only 4.3 cm³) needed by a conventional metal plate-type PIFA. Computed and measured bandwidth of the antenna indicates good performance for dual-band mobile phone application at around 900 and 1900 MHz.

A novel microstrip patch antenna with a Koch prefractal edge and a U-shaped slot as shown in Fig. 13, is proposed by Guterman et al [25] for multi-standard use in GSM1800, UMTS, and HiperLAN2. Making use of an inverted-F antenna (PIFA) structure an interesting size reduction is achieved.

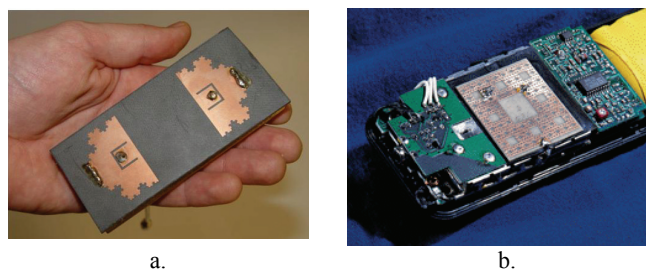


Fig. 13 The microstrip Koch fractal double-PIFA antenna photo for MIMO application [25] (a), and Sierpinski carpet fractal antenna in GPS handset by FRACTUS, Spain (b)

The two identical fractal PIFA elements have been disposed to ensure physical symmetry of the antenna structure, has been useful for MIMO applications. The antenna has been implemented in microstrip planar technology. A finite ground plane, of dimensions (100 x 45) mm, has been chosen to represent a common handset size. To obtain an additional miniaturization effect, the Koch-edge patch has been implemented in a PIFA configuration. By doing so, the patch

element length has been reduced by 62% in comparison with the simple rectangular patch. An example of Sierpinski carpet fractal antenna as applied inside the cellular phony handset is shown in Fig. 13b was made by FRACTUS, Spain.

IV. A NOVEL FRACTAL MULTIBAND EBG STRUCTURES

Ever-increasing demands for high-performance, low-profile, conformal and flush-mounted antennas with improved radiation characteristics for various communications and radar applications have resulted in considerable interest by the electromagnetic research community in high-impedance surfaces, also known as artificial magnetic conductors or metamaterials. Electromagnetic BandGap (EBG) materials [27] are periodic structures of notable interest for their applications both in the microwave region and millimeter-wave range. These surfaces have a reflection coefficient $\Gamma \cong +1$ when illuminated with a plane wave, instead of the typical $\Gamma \cong -1$ for a conventional perfectly electric conducting (PEC) surface. These structures can obviously offer interesting applications for antenna designs and for thin absorbing screens. For example, a horizontal dipole antenna placed above such a metamaterial surface will have an image current with the same phase as the current on the dipole, resulting in enhanced radiation performance. Several different types of high-impedance ground planes have been studied by various research groups.

Since magnetic conducting surfaces do not exist naturally, it is necessary to artificially create a surface with magnetic conduction properties in a certain band of frequencies. This can be achieved by utilizing resonant inclusions on a non-conducting host substrate layer in parallel with a conducting ground plane. Near the resonance of the inclusion, strong currents are induced on the surface, and together with the conducting ground plane, this structure may provide an equivalent magnetic conductor for a frequency range corresponding to the frequency range in the vicinity of a resonance of the surface. One possibility to form inclusions that are resonant but have an electrically small footprint at their resonant frequency is the use of the space-filling curves (e.g. Hilbert, Peano fractal curves).

An EBG structure can be considered as a stack of diffraction gratings separated by homogeneous layers. Engineered electromagnetic surface textures can be used to alter the properties of metal surfaces to perform a variety of functions. For example, specific textures can be designed to change the surface impedance for one or both polarizations, to manipulate the propagation of surface waves, or to control the reflection phase. These surfaces provide a way to design new boundary conditions for building electromagnetic structures, such as for varying the radiation patterns of small antennas. They can also be tuned, enabling electronic control of their electromagnetic properties. Tunable impedance surfaces can be used as simple steerable reflectors or as steerable leaky-wave antennas. The simplest example of a textured electromagnetic surface is a metal slab with quarter-wavelength deep corrugations [28], as shown in Fig. 14a.

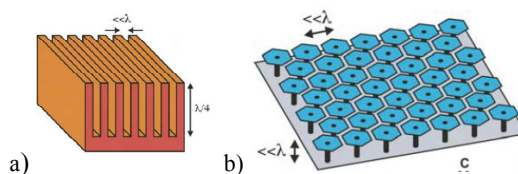


Fig. 14. A traditional corrugated surface (a), and a high-impedance surface built as thin two-dimensional lattice of plates attached to ground plane by metal-plated vias (b) [27]

This is often described as a soft or hard surface depending on the polarization and direction of propagation. It can be understood by considering the corrugations as quarter-wavelength transmission lines, in which the short circuit at the bottom of each groove is transformed into an open circuit at the top surface. This provides a high-impedance boundary condition for electric fields polarized perpendicular to the grooves and low impedance for parallel electric fields. Soft and hard surfaces are used in various applications, such as manipulating the radiation patterns of horn antennas or controlling the edge diffraction of reflectors. Two-dimensional structures have also been built, such as shorted rectangular waveguide arrays or the inverse structures, often known as pin-bed arrays. These textured surfaces are typically one-quarter-wavelength thick in order to achieve a high-impedance boundary condition.

Recently, compact structures have been developed that can also alter the electromagnetic boundary condition of a metal surface but which are much less than one-quarter-wavelength thick [29]. They are typically built as sub-wavelength mushroom-shaped metal protrusions, as shown in Figure 14b, or overlapping thumbtack-like structures. These materials provide a high-impedance boundary condition for both polarizations and for all propagation directions. They also reflect with a phase shift of zero, rather than π , as with an electric conductor. They are sometimes known as artificial magnetic conductors because the tangential magnetic field is zero at the surface, rather than the electric field, as with an electric conductor. In addition to their unusual reflection-phase properties, these materials have a surface wave bandgap, within which they do not support bound surface waves of either transverse magnetic (TM) or transverse electric (TE) polarization. They may be considered as a kind of electromagnetic bandgap (EBG) structure or photonic crystal for surface waves. Several broadband EBG structures were found in the literature. Typically, there have been two approaches aiming to obtain EBG structures with wider bandwidth: the use of EBGs with via-holes [29] (with the inconveniences of complex and expensive manufacturing process) and the adoption of multilayered FSSs over a metallic ground plane or multi-period mushroom-like structure (which yields less compact designs and is rather expensive). Recent research efforts focus on the development of planar EBG that does not need vias and that can be integrated antenna to enhance the gain and reduce the backward radiation and increasing efficiency [30].

With the growing interests in design of multi-band antennas in wireless communication system, it needs to invent corresponding multi-band EBG structures. It is natural to

think of fractals. The self-similarity property of fractal shapes, i.e., the replication of the geometry at different scales within the same structure, results in a multi-band behavior, making fractals especially suitable to design multi-frequency antennas [1]. The self-similarity property has also been exploited in the design of multi-band frequency selective surfaces in literature. In [31], EBG materials made of dielectric rods with fractal cross sections have been proposed and analyzed, showing multiband behaviour and enlargement of stop-band. Fractal geometry is successfully applied on uniplanar PBG structures. The fractal geometry is applied on a PVEBG (Pad and Via EBG) structure to achieve multi-frequency bandgap feature [32].

The construction of the fractal EBG unit cells is carried out by applying iterative processes on a simple starting topology. Referring to Fig. 15, this self-affine fractal shape (Fig.4b) begins as a simple rectangle whose iteration order is zero.

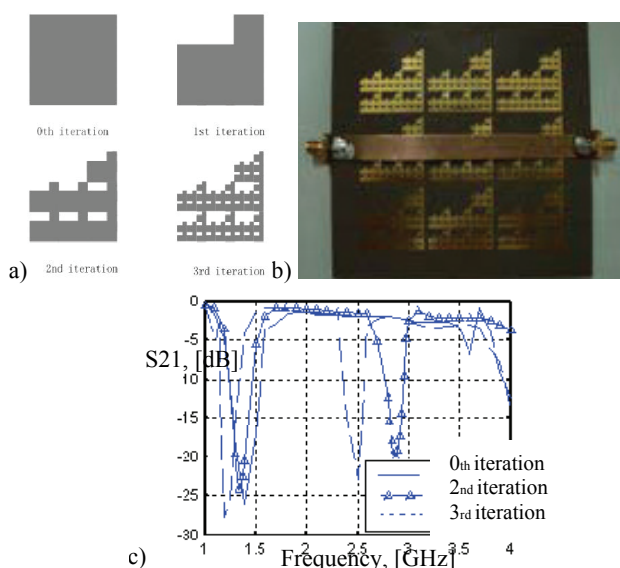


Fig. 15 Construction of the fractal EBG unit cell (a), photo of the fractal EBG with suspended microstrip (b), and simulated S_{21} of fractal EBG structures with different iterations (c) [32]

Next, divide it into nine identical small rectangles and remove the two squares in the blanks. One can iterate the same subtraction procedure on the remaining squares and if the iteration is carried out an infinite number of times, the ideal fractal geometry is obtained. Different fractal orders lead to different current paths. Thus the position of the second bandgap should be subject to the fractal order. To verify this, fractal geometry with the same starting topology but different fractal orders are designed and simulated. As shown in Fig. 15c, the central frequency of the second bandgap is decreased from 2.88GHz to 2.62GHz when the fractal order is changed from 2 to 3, which indicates that the frequency bandgap is tunable.

The novel hexagonal EBG structure was found by investigating in case of changing the gap between two adjacent Sierpinski triangles inside EBG unit cell [33]. As a result, two structures are proposed; in which one structure introduces broad bandwidth and the other introduce dual bandgap. The design of EBG structures involving the mode-2

Sierpinski gasket triangles (see Figure 16) and without vias or multilayer substrate is presented.

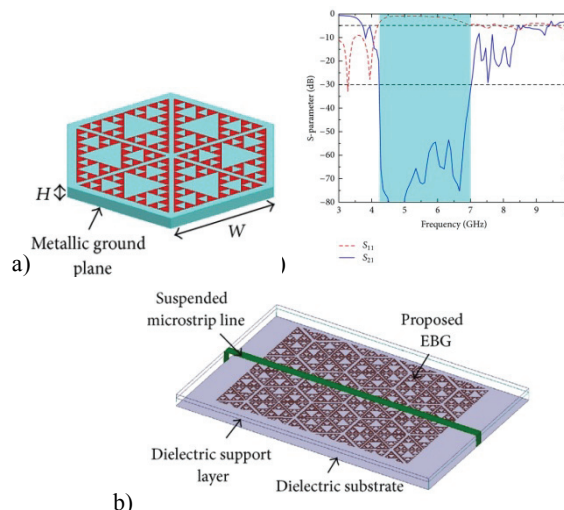


Fig. 16 Unit BEBG cell geometry (a), geometry of 3×4 array of hexagonal EBG structure based on Sierpinski triangle (b), and operation bandwidth of proposed array (c) [33]

Presented a novel EBG design using Sierpinski gasket triangles, which are arranged to repeat 60° to form the hexagonal EBG unit cell. The EBG structure, which has broadband bandgap, is proposed by setting the value of the gap between two adjacent Sierpinski inside the unit cell is equal to 0 mm. The bandwidth of BEBG structure is much larger than that of the conventional EBG. The results show a good agreement between simulations and measurements. Due to several advantages of the structures such as using inexpensive dielectric substrate FR4 and planar structure, the EBG structures are promising for low profile and low cost antennas in broadband or multiband applications.

V. CONCLUSION

Fractal EM engineering represents a relatively new field of research that combines attributes of fractal geometry with EM theory. Research in this area has recently yielded a rich class of new designs for antenna as well as metamaterials elements. Fractals are space-filling geometries that can be used as EM-devices to effectively fit long electrical lengths into small areas. This concept has been applied to wire and patch antennas and metamaterials element-structures. Antenna technology had to be revised to fulfil demands imposed by wireless systems, because conventional antenna technology can no longer meet future challenges. Fractal technology allows to be designed of smaller, high-performance, multiband devices. The design, development and manufacture of a fractal antenna and metamaterials for use in the ISM bands were presented. Using Zeland's, CST Microwave Studio and other antenna software, the engineer has the ability to perform end-to-end design simulations, avoiding costly prototypes. This allows the engineer to investigate more "what-if" designs, thereby increasing the likelihood of producing superior products that cost less and take less time to develop.

ACKNOWLEDGEMENT

This is an extended version of the paper "Take Advantage of Fractal Geometry in the Antenna Technology of Modern Communications" [26], presented at the 11th International Conference on Telecommunications in Modern Satellite, Cable and Broadcasting Services – TELSIS 2013, held in October 2013 in Niš, Serbia.

REFERENCES

- [1] W.J. Krzysztofik, *Printed Multiband Fractal Antennas. in: Multiband Integrated Antennas for 4G Terminals*, / ed. David A. Sanchez-Hernandez. Norwood, MA, USA: Artech House, INC., 2008.
- [2] W.J. Krzysztofik, "Modified Sierpinski Fractal Monopole for ISM Handset Applications", *IEEE Transaction on Antenna and Propagation*, 2009, t. 57, nr 3, 606-615
- [3] W.J. Krzysztofik, "Fractal Monopole Antenna for Dual-ISM-Bands Applications", *EuMC-2006, European Microwave Conference*, Manchester, UK, 2006, 1461-1464.
- [4] W.J. Krzysztofik, *Terminal Antennas of Mobile Communication Systems – Some Methods of Computational Analysis*, Wroclaw University of Technology Press, Wroclaw, Poland, 2011.
- [5] W.J. Krzysztofik, M. Baranski, *Fractal Structures in Antenna Technology*, Scientific Books of Gdansk University of Technology, Series: Radio Communication, Radiobroadcasting & Television, Gdansk, Poland, June 2007, vol. 1, 381-384.
- [6] W.J. Krzysztofik, "Fractal Antenna for WLAN/Bluetooth Multiple-Bands Applications", *EUCAP 2009, 3rd European Conference on Antennas and Propagation*, Berlin, Germany, 2009, 2407-2410.
- [7] W.J. Krzysztofik, M. Komaryczko, "Fractal Antennas in Terminals of Mobile Communication Systems", *KKRRIT-2004, National Conf. on Radio Communication, Radiobroadcasting & Television*, Warsaw, Poland, 2004, 436-439.
- [8] M.Z. Zaad, M. Ali, "A Miniature Hilbert PIFA for Dual-Band Mobile Wireless Applications", *IEEE Antennas and Wireless Propagation Letters*, vol. 4, 2005, pp. 59-62
- [9] S.R. Best, J.D. Morrow, "The Effectiveness of Space-Filling Fractal Geometry in Lowering Resonant Frequency", *IEEE Antennas and Wireless Propagation Letters*, vol. 1, 2002, pp. 112-115.
- [10] H.N. Kritikos, D.L. Jaggard (eds.), *Recent Advantages in Electromagnetic Theory*, New York: Springer-Verlag, 1990.
- [11] S.N. Sachendra, M. Jain, "A Self-Affine Multiband Antenna", *IEEE Antennas and Wireless Propagation Letters*, vol. 6, 2007, pp. 110-112.
- [12] K.J. Falconer, *Fractal Geometry: Mathematical Foundations and Applications*, Chichester, New York: John Wiley & Sons, 2nd ed., 2003.
- [13] B.B. Mandelbrot, *The Fractal Geometry of Nature*, New York: W.H. Freeman, 1983.
- [14] D.H. Werner, "Fractal Radiators", *Proceedings of the 4th Annual 1994 IEEE Mohawk Valley Section Dual-Use Technologies & Applications Conference*, vol. I, SUNY Institute of Technology at Utica/Rome, New York, May 23-26, 1994, pp. 478-482.
- [15] N. Cohen, *Fractal Antennas*, Communications Quarterly, Part 1, Summer, 1995, pp. 7-22, Part 2, Summer, 1996, pp. 53-66, Part 3, Spring, 1996, pp. 25-36, Winter 1996, pp. 77-81.
- [16] Y. Rahmat-Samii, J.P. Gianvittorio, "Fractal Antennas: A Novel Antenna Miniaturization Technique and Applications", *IEEE Antenna's and Propagation Magazine*, vol. 44, no. 1, February 2002, pp. 20-36.
- [17] C. Puente, C.P. Baliarda, J. Romeu, A. Cardama, "The Koch Monopole: A Small Fractal Antenna", *IEEE Transactions on Antennas and Propagation*, AP-48, 11, 2000, pp. 1773-81.
- [18] D.H. Werner, A.R. Bretones, B.R. Long. *Radiation Characteristics of Thin-Wire Ternary Fractal Trees*, Electronics Letters, 35, 8, 1999, pp. 609-10.
- [19] D.H. Werner, S. Gangul, "An Overview of Fractal Antenna Engineering Research", *IEEE Antennas and Propagation Magazine*, vol. 45, no. 1, February 2003, pp. 38-57.
- [20] C. Puente, J. Romeu, R. Pous, X. Garcia, F. Benitez, "Fractal Multiband Antenna Based on the Sierpinski Gasket", *IEEE Electronics Letters*, 32, 1, January 1996, pp. 1-2.
- [21] M. K. A. .Rahim, A. S. Jaafar, M. Z. A. A. Aziz, "Sierpinski Gasket Monopole Antenna Design", *2005 Asia-Pacific Conference on Applied Electromagnetic Proceedings*, December 20-21, Malaysia, pp. 49-52.
- [22] S.R. Best, *Operating Band Comparison of Perturbed Sierpinski and Modified Parany Gasket Antennas*, IEEE Antennas and Wireless Propagation Letters, vol. 1, 2002, pp. 35-38.
- [23] J. Anguera, C. Puente, C. Borja, J. Soler, *Fractal-Shaped Antennas: a Review*, Wiley Encyclopaedia of RF and Microwave Engineering, Edited by Professor Kai Chang, vol. 2, pp. 1620-1635, 2005.
- [24] K. Jaroniek, *Fractal Antenna of Multi-Mobile Systems Handset Terminal*, BSc Dissertation Diploma, Wroclaw University of Technology, Faculty of Electronic Engineering, Wroclaw, Poland, 2013.
- [25] J. Guterman, A.A. Mortira, C. Peixeiro, "Microstrip Fractal Antennas for Multistandard Terminals", *IEEE Antennas and Wireless Propagation Letters*, vol. 3, 2004, pp. 351-354.
- [26] W.J. Krzysztofik, "Take Advantage of Fractal Geometry in the Antenna Technology of Modern Communication", *TELSIS 2013, 11th International Conference on Telecommunications in Modern Satellite, Cable and Broadcasting Services*, 16-19 October 2013, Niš, Serbia, vol. 2, pp. 419-428.
- [27] N. Engheta, R. W. Ziolkowski, „Metamaterials. Physics and Engineering Explorations”, *IEEE Press*, Wiley-Interscience, John-Wiley & Sons, Inc., USA, 2006.
- [28] P.-S. Kildal, "Artificially soft and hard surfaces in electromagnetic", *IEEE Trans. Antennas Propag.*, vol. 38, pp. 1537-1544, June 1990.
- [29] D. Sievenpiper, L. Zhang, R. Broas, N. Alexopolous, E. Yablonovitch, "High-impedance Electromagnetic Surfaces with a Forbidden Frequency Band", *IEEE Trans. Microwave Theory Tech.*, vol. 47, pp. 2059-2074, Nov. 1999.
- [30] M.F. Abedin, M.Z. Azad, M. Ali, "Wideband smaller unit-cell planar EBG structure and their application," *IEEE Transactions on Antennas and Propagation*, vol. 56, no. 3, pp. 903-908, 2008.
- [31] F. Frezza, L. Pajewski, G. Schettini, *Fractal Two-Dimensional Electromagnetic Bandgap Structures*, *IEEE Trans. Microwave Theory & Tech.*, vol. 52, pp.220-226, Jan. 2004
- [32] Y. Wang, J. Huang, Z. Feng, "A Novel Fractal Multi-Band EBG Structure and Its Application in Multi-Antennas", *IEEE International Symposium Antennas and Propagation Society*, 2007, pp. 5447-5450.
- [33] H.N.B. Phuong, D.N. Chien, T.M. Tuan, "Novel Design of Electromagnetic Bandgap Using Fractal Geometry", *HINDAVI International Journal of Antennas and Propagation*, vol. 2013 (2013), Article ID 162396, 8 pages, <http://dx.doi.org/10.1155/2013/162396>